

CFD Modelling of Primary Atomisation of Diesel Spray

M. Ghiji¹, L. Goldsworthy¹, V. Garaniya¹, P.A. Brandner¹, and P. Hield²

¹Australian Maritime College, University of Tasmania, Launceston, Tasmania 7250, Australia

²Defence Science and Technology Organisation, Melbourne, Victoria 3010, Australia

Abstract

Primary atomisation in a high-pressure diesel jet is modelled using Large Eddy Simulation. The Volume Of Fluid phase-fraction based interface capturing technique was applied in the Eulerian framework using the open source CFD code OpenFOAM. Conditions modelled replicate those of a parallel experimental program including nozzle inlet pressure change, spray chamber pressure (ambient zone) and temperature and viscosity of both phases. The nozzle geometry was obtained using X-ray Computed Aided Tomography. Diesel fuel pressure at sac inlet was defined based on injection pressure profile (ranging from 30 to 1200 bar) captured during experimental tests. The effect of different grid sizes with mesh resolutions of 2.5, 8, and 18 million cells on primary breakup was investigated. The results assist with understanding the flow behaviour during primary break up, including commencement of fragmentation and the early spray cone angle. The results also showed that the jet break-up increased in meshes with higher resolutions. Furthermore, investigation of in-nozzle flow indicated a non-axisymmetric behaviour. The early spray angle of the numerical results was less than the experimental data, probably due to cavitation and compressibility not being modelled. These effects will be studied in forthcoming works.

Introduction

In diesel engines, combustion chambers are fed by high pressure fuel injected as a cone spray. This spray undergoes a series of instabilities (longitudinal and transverse) which lead to the fragmentation of the liquid bulk into liquid structures that further disintegrate into droplets. This initial process of atomisation is called the primary breakup and occurs in the vicinity of the injection point. The mechanisms of the primary breakup which initiate the atomisation process control the extent of the liquid core and provide initial conditions for secondary breakup in the dispersed flow region [3, 6, 7].

So far, many theories are proposed to describe the primary atomisation mechanisms, including:

- Aerodynamic shear forces which act through striping and Kelvin-Helmholtz instabilities [2, 7]
- Turbulence-induced disintegration which has significant effect in lower velocity jet breakup [4]
- Relaxation of the velocity profile, creating a “bursting” effect specially in non-cavitating jet and large velocity differentials [2]
- Cavitation-induced disintegration of the jet due to the reduction of cross-section area and collapse of cavitation bubbles at the nozzle inlet [2, 5]
- Liquid bulk oscillation provoking the toroidal surface perturbation [4].

It is difficult to separate and investigate these different effects experimentally [2-4]. To develop diesel engines with both

optimal fuel economy and reduced pollutant emissions, it is necessary to thoroughly understand the spray processes and then characterize the effects of different parameters and engine operating conditions on fuel flow structures. This is a challenging subject to study both experimentally and numerically.

There are two main physical phenomena involved inside the nozzle, cavitation and in-nozzle turbulence. This paper concentrates on the effect of in-nozzle turbulence. The effects of cavitation will be studied in future work. Turbulent flows are represented by eddies with ranges of length and time scales. Large eddy simulation (LES) directly resolves large scales and models small scales. Modelling only small scales and solving the large scales, allows the use of a much coarser mesh and larger time steps in LES compared with Direct Numerical Simulation (DNS). Despite this, LES still needs a finer mesh compared with the ones used for Reynolds Averaged Navier Stokes (RANS) computations. Since RANS models cannot capture the transient spray structure [3, 7], including droplet clustering and shot to shot variability, LES is applied to overcome these limitations.

Reviews of the existing atomisation models demonstrated that all these models (blob, Huh/Gosman, MPI, Arcoumanis, Nishimura, V.Berg, Baumgarten, ReitzWave model, Taylor Analogy Breakup model) simplify the droplet generation in the dense region (primary atomisation) resulting in inaccurate and unrealistic simulations [3, 9]. For example, the blob atomisation model which is the most employed model not only simply generates parcels with the size of the nozzle diameter but also does not take into account the physics of in-nozzle turbulence and in-nozzle cavitation. In addition, these conventional atomisation models with Lagrangian Particle Tracking (LPT) limit the grid fineness near the nozzle and do not allow LES to capture the features of the spray and background fluid flow near the nozzle. Refining the grid creates problems in the LPT approach due to the high liquid fraction in each cell [9]. These limitations motivate the development of a new method to model the primary atomisation using the Eulerian/ Volume of Fluid (VOF)/LES approach, instead of using the conventional atomisation model. In this study, the flow inside the nozzle and the liquid bulk near the nozzle exit and its fragmentation (primary atomisation) in a non-evaporating spray in a chamber are analysed.

Methodology

Mathematical Method

In this study, the VOF phase-fraction based interface capturing technique is used in an open source CFD code OpenFOAM v2.1. This code considers the two-phase flow field as a single incompressible continuum with constant ρ and viscosity μ , including surface tension forces. The compressibility effect is not included in the present study but will be considered in future studies. Governing mass and momentum conservation equations used are:

$$\nabla \cdot \mathbf{V} = 0 \quad (1)$$

$$\frac{\partial \rho V}{\partial t} + \nabla \cdot (\rho V V) = -\nabla p + \nabla \cdot \tau + \int_{S(t)} \sigma k' n' \delta(x - x') dS \quad (2)$$

Where V is the velocity, p is the pressure, t is the time and τ is the viscous stress tensor, given by the Newtonian constitutive equation. The last term of equation (2) is the force caused by surface tension. This force only applies on the phase interface (S), as indicated by $\delta(\cdot)$ function. n is the unit vector normal to S , with local curvature of κ . The time-varying phase interface $S(t)$ is captured and tracked using a VOF surface-capturing method, which uses the volume fraction γ of the diesel fuel as an indicator function described as:

$$\gamma = \begin{cases} 1 & \text{for a point inside the liquid} \\ 0 < \gamma < 1 & \text{for a point in the transitional region} \\ 0 & \text{for a point inside the gas} \end{cases} \quad (3)$$

The indicator function, being a Lagrangian invariant, obeys a transport equation of the form [4]

$$\frac{\partial \gamma}{\partial t} + \nabla \cdot (V \gamma) = 0 \quad (4)$$

Using equation (3), the local density and viscosity of the spray are calculated by:

$$\rho = \gamma \rho_f + (1 - \gamma) \rho_g \quad (5)$$

$$\mu = \gamma \mu_f + (1 - \gamma) \mu_g \quad (6)$$

Where ρ and μ are the density and viscosity of diesel/air mixture. The indexes f and g represent the liquid and gas respectively.

The LES/VOF equations are extracted from equation (2) via a filtering process of the phase-weighted properties. This process decomposes the dependent variables into resolvable and sub-grid scales (SGS) of turbulent fluctuations and consequently eliminates the sub-grid scale motions from direct simulation. This process introduces an additional term named subgrid scale stresses τ^{sgs} in filtered momentum equation, which represents the effect of the unsolved small scales of turbulence:

$$\tau^{sgs} = \overline{V V} - \overline{V} \overline{V} \quad (7)$$

The above form can be calculated by an eddy-viscosity type of single subgrid model as:

$$\tau^{sgs} - \frac{2}{3} k I = -\frac{\mu^{sgs}}{\rho} (\nabla \overline{V} + \nabla \overline{V}^T) \quad (8)$$

where k is the subgrid scale turbulent energy and μ_{sgs} is the subgrid scale viscosity, computed from the one-equation SGS turbulent energy transport model accredited to Yoshizawa [11].

$$\frac{\partial k}{\partial t} + \nabla \cdot (k \overline{V}) = \nabla \cdot [(\vartheta - \vartheta^{sgs}) \nabla k + \tau^{sgs} \cdot \overline{V}] - \varepsilon - \frac{1}{2} \tau^{sgs} : (\nabla \overline{V} + \nabla \overline{V}^T) \quad (9)$$

Where $\varepsilon = C_k k^{2/3} / \Delta$ is the SGS turbulent dissipation, $\vartheta^{sgs} = C_k k^{1/2} / \Delta$ and Δ is the SGS length scale, defined as $\Delta = \sqrt[3]{V}$ where V is volume of the computational cell. The coefficients are $C_k = 0.05$ and $C_\varepsilon = 1$ [9].

The Numerical Solution Method

The mathematical model for the atomisation simulation is solved using an implicit finite-volume method and employs second-order spatial and temporal discretisation schemes. The solution procedure employed uses the Pressure Implicit with Split Operator (PISO) algorithm, in conjunction with conjugate gradient methods.

Boundary Conditions and Initial Set up

Atomisation is affected by the shape of the sac and the design of inlet nozzle hole [7]. The computational domain has therefore

been modelled using the geometry of the experimental nozzle determined using X-ray Computed Aided Tomography (CAT) analysis as shown in Figure 1.

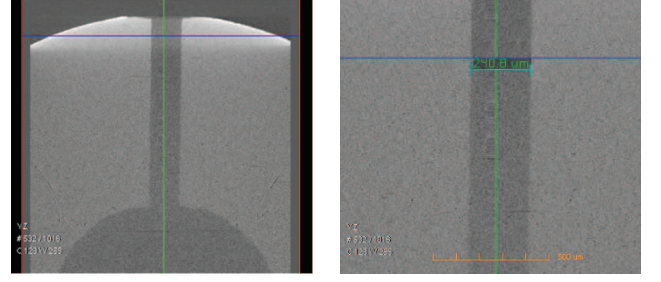


Figure 1. X-Ray Tomography results showing dimensions of the sac and nozzle hole diameter. Left: X-Z view and Right: Y-Z zoomed view of the nozzle hole

All experimental conditions replicated in numerical models were based on the previous study by Bong et al. [3] including diesel fuel pressure at the sac volume inlet, spray chamber pressure and air and diesel fuel temperature and viscosity. This study was performed using a single solid cone diesel injector in the constant volume High-Pressure Spray Chamber (HPSC), at Australian Maritime College (AMC). Micro spray structure and physics of the spray were studied by shadowgraphy employing a long range microscope along the atomisation zone. Fuel properties and setup conditions used in the simulations are described in Table 1.

Parameter	Value
Injection pressure	120 MPa average
Nozzle diameter	0.24 mm
Nozzle length	1.6 mm
Fuel	Diesel
Diesel fuel density	832 kg/m ³
Gas	Compressed air
Density ratio	42
Kinematic viscosity	2.41 × 10 ⁻⁶ m ² /s
Surface tension	0.03 N/m
Temperature	25 °C
Injection duration	Up to 17 ms
Reynolds Number	33310
Mach number of fuel	0.3
Mach number of air	1.07
Weber number	896400
Ohnesorge number	0.077
Chamber pressure	30 bar

Table 1. Fuel properties and operating conditions based on experimental setup [6]

To initialize the simulation, the sac volume and three quarters of the orifice were filled with diesel fuel with a pressure of 30 bar, matching the experimentally measured injector pressure profile. A hexahedral structured mesh was generated as shown in Figure 2, with mesh refinement in the boundary layers (sac and orifice walls) and the atomisation zone. It has been shown that the spray structure is not axisymmetric [3, 6], so the full 360° of the atomisation zone has been meshed. In order to perform a mesh dependency study, different mesh resolutions were produced with coarse (2.5×10⁶ cells), medium (8×10⁶ cells) and fine (18×10⁶ cells) resolutions. The cell size was refined to 1 μm in the primary atomisation zone and near nozzle wall in the finest resolution case (18×10⁶ cells) as shown in Figure 2.

This cell size can capture droplets down to 2 μm range based on the optimistic premise that 2-3 cells can give reasonable representation of a single droplet. The resolutions of these three cases is summarised in Table 2.

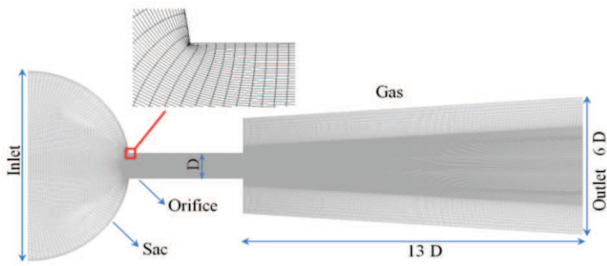


Figure 2. Calculation domain and boundary conditions (refined mesh in atomisation and nozzle hole)

Case	Resolution	Cell count
Coarse	5 μm	2.5×10^6
Medium	3 μm	8×10^6
Fine	1 μm	18×10^6

Table 2. Resolution and cell count of three cases for mesh study.

Results

The turbulent eddies produced within boundary layers inside the orifice lead to small/large-scale irregularities, which are considered to be the origin of initial jet surface instabilities. Figure 3 illustrates the enlarged view of velocity profile inside the nozzle hole for three cases which depict smaller-scale irregularities in cases with higher mesh resolution.

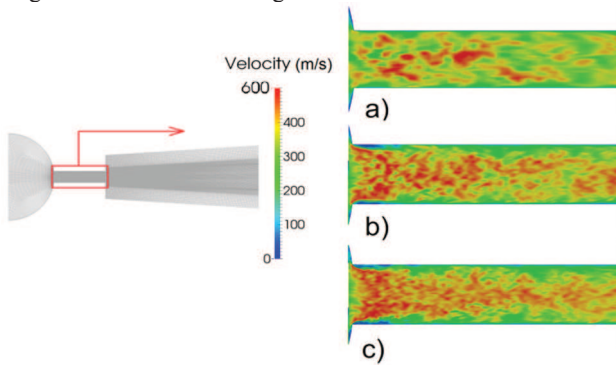


Figure 3. The velocity magnitude of jet inside the nozzle hole at $t = 1$ ms and $P = 1200$ bar for (a) Coarse, (b) Medium and (c) Fine mesh

The general spray structure is illustrated in Figure 4 by $\gamma=0.1$ iso-surfaces, showing the velocity magnitude plotted in the axial plane at 1 ms after the Start Of Injection (SOI) where the diesel fuel pressure at the sac inlet is 1200 bar for the three different cases. The onset of primary atomisation can be seen to occur close to the nozzle exit for the three different mesh resolutions. Progressively finer droplets are captured near the nozzle exit with increasing mesh density most noticeably for the finest case (18 M cell). In-nozzle-generated turbulence in combination with relaxation of the velocity profile at nozzle exit initiates the perturbations leading to amplification of surface waves. The number of droplets considerably increases while the droplet diameter decreases with increasing mesh resolution. This is due to better prediction of the small-scale turbulent structures within the nozzle hole as presented in figure 4, resulting in smaller-scale structures on the jet surface. These instabilities develop into finer clusters and intensify the break up process. Consequently, the rate of break up increases in cases with higher mesh resolution.

The growth of non-axisymmetric disintegration at different cross-sections from the nozzle orifice exit is presented in Figure 5. As seen, the formation of small waves is obvious even 1 nozzle diameter downstream of the nozzle exit. Primary break up triggers and intensifies after $x/d = 1$. This can question the ability of any conventional atomisation models [9] which don't predict small droplet generation close to the nozzle exit. Up to 5 diameters ($x/d = 5$) downstream of the nozzle exit the breakup process is fully developed since the liquid core is narrowing to

tapered ligaments. This liquid core is totally disintegrated at 8 diameters ($x/d=8$) downstream, resulting in a high number of droplets.

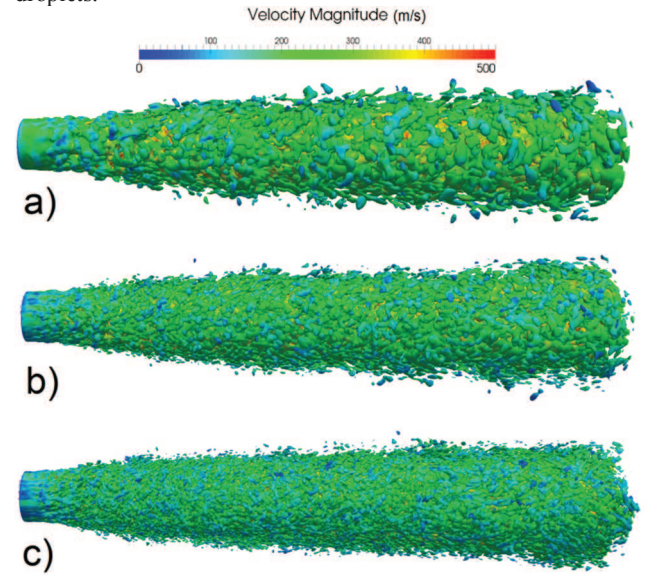


Figure 4. Morphology of the spray coloured by velocity magnitude at $t = 1$ ms and $P = 1200$ bar in sac volume inlet, indicated by iso-surfaces of volume fraction $\gamma = 0.1$, (a) Coarse, (b) Medium and (c) Fine cases.

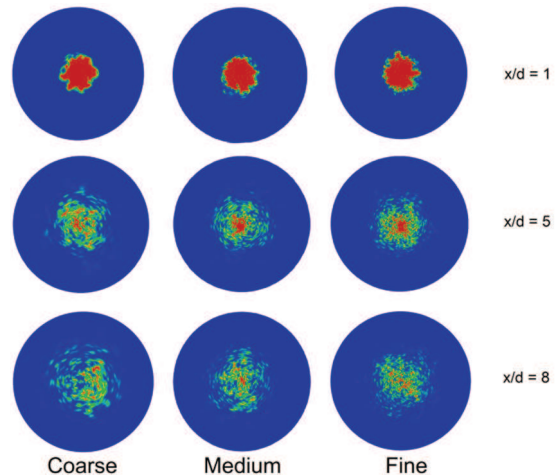


Figure 5. In-nozzle liquid distribution in cross-sectional planes at different axial positions for Coarse (Right column), Medium (Middle column) and Fine (Left column) cases at $t = 1$ ms and $P = 1200$ bar in sac inlet

Figure 6 shows the measured early spray angle at $t=1$ ms after SOI where the formation and development of shear layer instabilities can be clearly seen. The end of the nozzle is apparent in the left side of the picture.

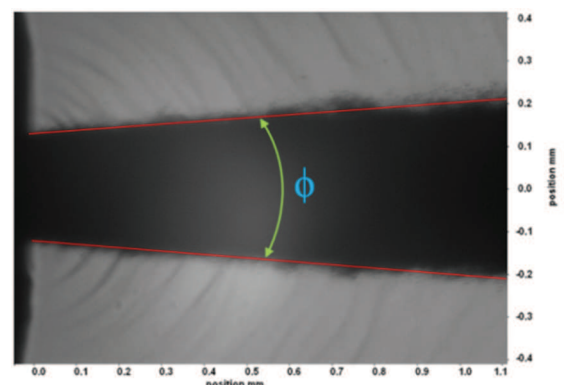


Figure 6. Shadowgraphy of the diesel spray at $t=1$ ms after SOI using long distance microscope [6].

To compare the early spray angle of the numerical simulation with the experimental results, Leboissetier and Zaleski [10] core analysis was conducted. Based on this method, three different zones were distinguished at every time step during the fully developed state. The result of this analysis for three different cases is depicted in Figure 7, showing the time-averaged structure of the atomisation region. The red zone contains only liquid (never contains gas), so that represents the liquid core; blue region experiences just gas while the green region contains sporadically liquid or gas and therefore depicts the atomisation zone. The early spray angle was extracted using an outer boundary of the two phase mixture (green) zone.

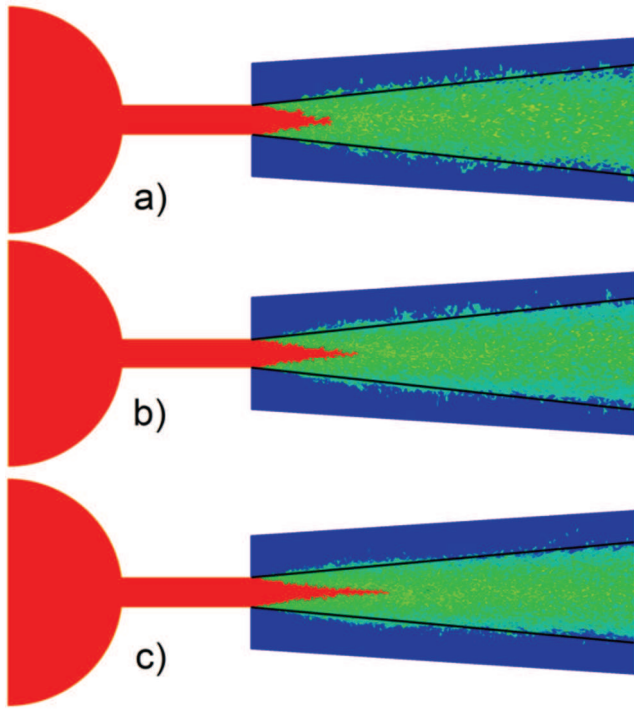


Figure 7. Spray angle and core analysis, (a) Coarse (b) Medium (c) Fine. The red zone represents the liquid core; blue region experienced just gas and green region depicts the atomisation zone.

The summary of this work is listed in Table 3, which shows a reduction in spray angle and an increase in liquid core length for the higher resolution cases. The spray angle is over predicted in comparison with experimental data. These variations could be due to cavitation and compressibility effects which were not included in this study. KS Im et al. [8] demonstrated that cavitation plays a significant role in determining the spray angle by reducing the jet diameter.

Preliminary results of diesel spray simulations including the effects of compressibility show an influence on the spray angle. It has also been shown that cavitation occurs along the entire nozzle length which will have a significant impact on the spray. Simulations including both compressibility and cavitation will be published in forthcoming journal papers.

Case	Early Spray Angle (ϕ)	Core Length (mm)
Experiment [6]	$8.7 \pm 0.4^\circ$	-
Coarse	$12.21 \pm 1^\circ$	0.73
Medium	$11.58 \pm 0.8^\circ$	0.93
Fine	$10.16 \pm 0.5^\circ$	1.18
Arai [1]	-	1.21

Table 3. Comparison of spray angle and liquid core length

Conclusions

General structure of primary atomisation of diesel sprays was successfully characterized using CFD methodology which

employed the Eulerian/LES/VOF approach to capture the free surface. A mesh resolution study revealed that:

- Mesh independence has not been demonstrated
- Fragmentation of the jet commenced close to the nozzle exit (about 1 diameter from exit)
- The primary breakup process enhances for cases with higher resolution
- The size of droplets decreases for the higher cell resolution.
- Smaller eddies were captured by decreasing size of cells inside the nozzle
- Increasing mesh resolution leads to decrease in the early spray angle and increase in the liquid core length

The over-prediction of early spray angle and under-prediction of liquid core length might be due to not including cavitation and compressibility which will be examined in future studies.

Acknowledgments

The authors wish to acknowledge the support of the Australian Maritime College and the Defence Science and Technology Organisation (DSTO). The authors express their gratitude to other partners in the project for their support and suggestions.

References

- [1] Arai, M., Tabata, M., Hiroyasu, H. & Shimizu, M., Disintegrating process and spray characterization of fuel jet injected by a diesel nozzle, *SAE Technical Paper*, No. 840275, 1984.
- [2] Baumgarten, C., *Mixture formation in internal combustion engines*, Springer, 2006.
- [3] Bong, C.H., *Numerical and experimental analysis of diesel spray dynamics including the effects of fuel viscosity*, University of Tasmania, 2010.
- [4] de Villiers, E., Gosman, A. & Weller, H., Large eddy simulation of primary diesel spray atomization, *SAE transactions*, **113**, 2004, 193-206.
- [5] Giannadakis, E., Gavaises, M. & Arcoumanis, C., Modelling of cavitation in diesel injector nozzles, *Journal of Fluid Mechanics*, **616**, 2008, 153-193.
- [6] Goldsworthy, L., Bong, C.H. & Brandner, P.A., Measurements of diesel spray dynamics and the influence of fuel viscosity using PIV and shadowgraphy, *Atomization and Sprays*, **21**, No.2, 2011.
- [7] Gorokhovski, M. & M. Herrmann, Modeling primary atomization, *Annu. Rev. Fluid Mech*, **40**, 2008, 343-366.
- [8] Im, K. S., Cheong, S. K., Powell, C. F., Ming-chia, D. L., & Wang, J., Unraveling the Geometry Dependence of In-Nozzle Cavitation in High-Pressure Injectors, *Scientific reports*, **3**, 2013.
- [9] Kaario, O., Vuorinen, V., Hulkkonen, T., Keskinen, K., Nuutinen, M., Larmi, M. & Tanner, F. X., Large Eddy Simulation of High Gas Density Effects in Fuel Sprays, *Atomization and Sprays*, **23**, No.4, 2013.
- [10] Scardovelli, R. & Zaleski, S., Direct numerical simulation of free-surface and interfacial flow, *Annual Review of Fluid Mechanics*, **31**, No.1, 1999, 567-603.
- [11] Yoshizawa, A. & Horiuti, K., A statistically-derived subgrid-scale kinetic energy model for the large-eddy simulation of turbulent flows, *Journal of the Physical Society of Japan*, **54**, No.8, 1985, 2834-2839.